THE JOURNAL OF BIOLOGICAL CHEMISTRY VOL. 289, NO. 1, pp. 89–99, January 3, 2014

Evaluation of the BH3-only Protein Puma as a Direct Bak Activator*[S]

Received for publication, July 29, 2013, and in revised form, November 13, 2013 Published, JBC Papers in Press, November 21, 2013, DOI 10.1074/jbc.M113.505701

Haiming Dai[‡], Yuan-Ping Pang[§], Marina Ramirez-Alvarado[¶], and Scott H. Kaufmann[‡§1]

From the [‡]Division of Oncology Research and Departments of [§]Molecular Pharmacology and Experimental Therapeutics and [¶]Biochemistry and Molecular Biology, Mayo Clinic, Rochester, Minnesota 55905

Background: How the DNA damage-induced proapoptotic protein Puma triggers apoptosis has been unclear.
Results: The Puma BH3 domain not only binds the Bak BH3 binding pocket with nanomolar affinity, but mutations affecting this binding alter Bak oligomerization, membrane permeabilization, and killing.
Conclusion: Puma is a direct Bak activator.
Significance: These observations help resolve a long-standing debate over the Puma role in apoptosis.

Interactions among Bcl-2 family proteins play critical roles in cellular life and death decisions. Previous studies have established the BH3-only proteins Bim, tBid, and Noxa as "direct activators" that are able to directly initiate the oligomerization and activation of Bak and/or Bax. Earlier studies of Puma have yielded equivocal results, with some concluding that it also acts as a direct activator and other studies suggesting that it acts solely as a sensitizer BH3-only protein. In the present study we examined the interaction of Puma BH3 domain or full-length protein with Bak by surface plasmon resonance, assessed Bak oligomerization status by cross-linking followed by immunoblotting, evaluated the ability of the Puma BH3 domain to induce Bak-mediated permeabilization of liposomes and mitochondria, and determined the effect of wild type and mutant Puma on cell viability in a variety of cellular contexts. Results of this analysis demonstrate high affinity ($K_D = 26 \pm 5$ nM) binding of the Puma BH3 domain to purified Bak *ex vivo*, leading to Bak homo-oligomerization and membrane permeabilization. Mutations in Puma that inhibit (L141E/M144E/L148E) or enhance (M144I/A145G) Puma BH3 binding to Bak also produce corresponding alterations in Bak oligomerization, Bak-mediated membrane permeabilization and, in a cellular context, Bak-mediated killing. Collectively, these results provide strong evidence that Puma, like Bim, Noxa, and tBid, is able to act as a direct Bak activator.

Apoptosis is a morphologically and biochemically distinct form of cell death that occurs under a variety of physiological and pathological conditions (1, 2) Although caspase-independent apoptosis has been described (3–5), apoptosis typically reflects the concerted action of effector caspases on hundreds of cellular substrates (6, 7). Three distinct pathways for activating these effector caspases have been described: a death receptor pathway that is triggered when certain tumor necrosis factor-α family members bind their receptors (8–12), granzyme B-mediated caspase activation triggered when cytotoxic lymphocytes and natural killer cells release contents of their lytic granules into the cytoplasm of target cells (13, 14), and a mitochondrial pathway that is activated when the mitochondrial outer membrane is breached and cytochrome *c* leaks into the cytoplasm, where it serves as a cofactor for Apaf-1-mediated caspase 9 activation (6, 15–18).

Previous studies have demonstrated that mitochondrial pathway activation results from protein-protein interactions involving members of the Bcl-2 family (15, 16, 18–20). Several pro-apoptotic family members, including Bax and Bak, are capable of directly permeabilizing mitochondria (21) or liposomes composed of mitochondrial outer membrane lipids (22, 23). These proteins are bound and inhibited by antiapoptotic paralogs, including Bcl-2 itself as well as Bcl-x_L, Mcl-1, Bcl-2 A1, and Bcl-w. The outcome of interactions between the Bax/Bak subfamily and the antiapoptotic Bcl-2 family members is in turn modulated by BH3[2]-only proteins, which share a 9–15-amino acid BH3 domain with other Bcl-2 family proteins (24). Some of these BH3-only proteins (termed direct activators) are thought to directly activate Bax and/or Bak, whereas others (termed "sensitizers") are thought to influence events by binding and neutralizing some or all of the antiapoptotic Bcl-2 family members (18, 19, 25, 26).

Previous assays that evaluated whether BH3-only proteins are direct activators or sensitizers (23) typically measured the ability of these proteins or their BH3 domains to modulate Bax-mediated release of fluorescently tagged macromolecules from liposomes composed of mitochondrial outer membrane lipids in the absence of other proteins (direct activators) or in the presence of Bcl-x_L and truncated Bid (sensitizers). Based on these assays, Bim and truncated Bid were identified as direct activators, whereas Bad was classified as a sensitizer (23).

* This work was supported, in whole or in part, by National Institutes of Health Grant R01 CA166704.
[S] This article contains supplemental Figs. S1–S6.
[1] To whom correspondence should be addressed: Division of Oncology Research, Gonda 19-212, Mayo Clinic, 200 First St., S.W., Rochester, MN 55905. Tel.: 507-284-8950; Fax: 507-293-0107; E-mail: Kaufmann.scott@mayo.edu.

[2] The abbreviations used are: BH, Bcl-2 homology; Q-VD-OPh, (3S)-5-(2,6-difluorophenoxy)-3-[[(2S)-3-methyl-1-oxo-2-[(2-quinolinylcarbonyl)-amino]butyl] amino]-4-oxo-pentanoic acid; BMH, bismaleimidohexane; EGFP, enhanced GFP; FACS, fluorescence-activated cell sorting; F-d10, fluorescein isothiocyanate-labeled dextran 10; SPR, surface plasmon resonance; MEF, mouse embryonic fibroblast; APC, allophycocyanin.

At present there is less consensus regarding the role of Puma. Originally identified as the BH3 domain-containing protein product of a p53 target gene (27, 28), Puma has been shown to play a critical role in apoptosis induced in many cell types by DNA damage (29–38), glucocorticoid treatment (29), cytokine withdrawal (30, 39–41), oncogene activation (30, 42–44), or treatment with various toxins (45–48) as well as death of lymphocytes after activation (49–51). Targeted deletion of the *Puma* gene also worsened the phenotype of *Bim*/*Bid* double knock-out mice, highlighting the importance of Puma to apoptotic processes (52). Because the Puma BH3 peptide did not enhance Bax-mediated liposome release in the initial studies (23), Puma was originally classified as sensitizer. Consistent with this classification, further studies demonstrated that Puma requires cooperation of the direct activator Bim or truncated Bid to induce apoptosis (53, 54). Alternatively, Puma was reported to displace the oncoprotein p53 from Bcl-x_L (55), leading to p53-mediated apoptosis. A separate line of investigation, however, suggested that Puma binds to the N-terminal α-helix of Bax (56–58), either promoting Bax translocation to mitochondria (59) or interacting with Bax at the mitochondrial outer membrane (60). In addition, some of the same investigators involved in the original classification reported that the Puma BH3 peptide weakly facilitates Bax-mediated liposome permeabilization (61), illustrating the potential difficulty in classifying BH3-only proteins solely with this assay.

Like Puma, Noxa was originally described as a sensitizer BH3-only protein based on liposome permeabilization experiments (21, 23). Our recent studies, however, utilized a wider range of assays, including surface plasmon resonance, cross-linking of Bak oligomers, and transient transfection of fibroblasts engineered to express wild type Bak or Bak mutated in the BH3-binding groove to study the role of Noxa during apoptosis (62). These studies demonstrated that a tight but transient interaction between the Noxa BH3 peptide and the latent BH3 binding groove of Bak leads to Bak oligomerization and activation, resulting in mitochondrial outer membrane permeabilization under cell-free conditions and killing of Bak-expressing cells (62). These studies led to the conclusion that Noxa is a direct activator of Bak, which has been independently confirmed (63). In the present study we have utilized a similar approach to assess whether Puma is also a Bak direct activator and map the sites of interaction between Puma and Bak.

EXPERIMENTAL PROCEDURES

Materials—Reagents were obtained from the following suppliers: lipids and extruder from Avanti Polar Lipids, CM5 biosensor chips from GE Healthcare, Polysorbate 20 from Biacore AB, Q-VD-OPh from SM Biochemicals (Anaheim, CA), glutathione from Sigma, glutathione-agarose and bismaleimidohexane (BMH) from Thermo Scientific, S protein-agarose and Ni^{2+}-nitrilotriacetic acid-agarose from Novagen, and FITC-labeled dextran 10 (F-d10) from Invitrogen. Antibodies to the following antigens were purchased from the indicated suppliers: heat shock protein 60 (Hsp60), Bax and green fluorescent protein (GFP) from Cell Signaling Technology, cytochrome *c* from BD Biosciences, Bak from Millipore, and β-actin (goat polyclonal) from Santa Cruz Biotechnology. Anti-S peptide antibody was raised in our laboratory as described (64). BH3 peptides were generated by solid phase synthesis in the Mayo Clinic Proteomics Research Center (Rochester, MN).

Protein Expression and Purification—Plasmids encoding BakΔTM (GenBank™ BC004431, residues 1–186) in pET29b(+) and pGEX-4T-1 (65) were kind gifts from Qian Liu and Kalle Gehring (McGill University, Montreal, Canada). Plasmids encoding Bak mutants were generated by site-directed mutagenesis. All plasmids were subjected to automated sequencing to verify the described alteration and confirm that no additional mutations were present.

To express Pumaα in *Escherichia coli*, cDNA encoding full-length Pumaα (GenBank™ NM_001127242) was cloned into pET29a(+) to yield a construct with an N-terminal S peptide tag and C-terminal His_6 tag. To improve expression in *E. coli*, rare codons, including codons for proline (CCC) and arginine (AGG, AGA), were mutated to more commonly used synonymous codons by site-directed mutagenesis. The plasmid was subjected to automated sequencing to verify the described alterations.

Plasmids were transformed into *E. coli* BL21 (DE3) by heat shock. After cells were grown to an optical density of 0.8, isopropyl 1-thio-β-D-galactopyranoside was added to 1 mM, and incubation was continued for 24 h at 16 °C. Bacteria were then washed and sonicated intermittently on ice in TS buffer (150 mM NaCl containing 10 mM Tris-HCl (pH 7.4) and 1 mM PMSF). All further steps were performed at 4 °C.

His_6-tagged proteins were applied to Ni^{2+}-nitrilotriacetic acid-agarose. After columns were washed with 20 volumes of TS buffer followed by 10 volumes TS buffer containing 40 mM imidazole, proteins were eluted with TS buffer containing 200 mM imidazole.

GST-tagged proteins were incubated with glutathione-agarose overnight at 4 °C. Beads were then washed twice with 20–25 volumes of TS buffer and eluted with TS containing 20 mM reduced glutathione for 30 min at 4 °C.

Surface Plasmon Resonance (SPR) Analysis—Proteins for SPR analysis were further purified by FPLC on Superdex S200 column, concentrated in a centrifugal concentrator (Centricon, Millipore), dialyzed against Biacore buffer (10 mM HEPES (pH 7.4), 150 mM NaCl, 0.05 mM EDTA, and 0.005% (w/v) Polysorbate 20), and stored at 4 °C for <48 h before use.

Puma BH3 peptide or Puma protein was immobilized on a CM5 chip using a Biacore T200 biosensor. Binding assays were performed at 25 °C using Biacore buffer containing GST or GST-BakΔTM (wt or mutant) injected at 30 μl/min for 1 min. Bound protein was allowed to dissociate in Biacore buffer at 30 μl/min for 10 min and then desorbed with 2 M $MgCl_2$. Binding kinetics were derived using BIAevaluation software (Biacore, Uppsala, Sweden). Similarly, His_6-tagged BakΔTM on a CM5 chip was exposed to Bim BH3, Puma BH3, Bad BH3, and Puma BH3 wild type peptide or mutants.

Preparation of FITC-Dextran Lipid Vesicles—1-Palmitoyl-2-oleoyl-*sn*-glycero-3-phosphocholine, 1-plamitoyl-2-oleoyl-*sn*-glycero-3-phosphoethan-olamine, L-α-phosphatidylinositol, cardiolipin, cholesterol, and 18:1 DGS-nitrilotriacetic acid (Ni^{2+}) at a weight ratio of 36:22:9:8:20:5 were dried as thin films in glass test tubes under nitrogen and then under vacuum for 16 h. To encapsu-

late FITC-labeled dextran 10 (F-d10), 50 mg of lipid in 1 ml of 20 mM HEPES, 150 KCl (pH 7.0) buffer was mixed with 50 mg of F-d10, sonicated, and extruded 15 times through a 100-nm polycarbonate membrane. Untrapped F-d10 was removed by gel filtration on Sephacryl S-300 HR (GE Healthcare). Phosphate was determined by colorimetric assay (Abcam, Cambridge, UK).

Liposome Release Assay (Modified from Oh et al. (66))—Release of F-d10 from large unilamellar vesicles was monitored by fluorescence dequenching using a fluorimetric plate reader. After purified His_6-BakΔTM together with BH3 peptides was added to large unilamellar vesicles (final lipid concentration 10 μg/ml), 96-well plates were incubated at 37 °C with mixing and assayed (excitation 485 nm, emission 538 nm) every 10 s. F-d10 release was quantified by the equation $((F_{sample} - F_{blank})/(F_{Triton} - F_{blank}) \times 100\%)$, where F_{sample}, F_{blank}, and F_{Triton} are fluorescence of reagent-, buffer-, and 1% Triton-treated large unilamellar vesicles.

BMH Cross-linking Assay—50 nM His_6-BakΔTM together with 200 nM BH3 peptides were incubated with large unilamellar vesicles at 37 °C for 30 min. BMH was then added to a final concentration of 100 μM, and cross-linking was allowed to proceed at 23 °C for 30 min. After the reaction was stopped by incubation with 5 mM DTT for 15 min, samples were diluted in SDS sample buffer, separated on a 12% SDS-polyacrylamide gel, transferred to nitrocellulose, and probed with anti-Bak antibody.

Analytical Gel Filtration—Purified His_6-tagged Bak C14S/C166S (20 μM) with or without the indicated BH3 peptide (60 μM) was incubated in CHAPS buffer (2% CHAPS, 150 mM NaCl, 20 mM HEPES (pH 7.5)) at 23 °C for 3 h. After 200-μl samples were injected onto a Superdex S200 size exclusion column, 500-μl fractions were collected, subjected to SDS-PAGE, and blotted with anti-Bak antibody. Molecular markers (Sigma) in the same buffer were also separated on the same column.

Cytochrome c Release—His_6-BakΔTM was dialyzed against mitochondria buffer (150 mM KCl, 5 mM $MgCl_2$, 1 mM EGTA, 25 mM HEPES (pH 7.5)) and diluted into mitochondria buffer with 5 mM DTT. Mitochondria purified from $Bak^{-/-}Bax^{-/-}$ MEFs (67) were incubated with His_6-BakΔTM and the indicated BH3 peptides at 23 °C for 2 h. After centrifugation (10,000 × *g*, 15 min), supernatants and pellets were analyzed by immunoblotting.

Cell Culture—Jurkat (T cell ALL) from Paul Leibson (Mayo Clinic, Rochester, MN) and SKW 6.4 (Epstein Barr virus-transformed lymphoma) from American Type Culture Collection were maintained at densities below 10^6 cells/ml in RPMI 1640 medium containing 10% heat-inactivated fetal bovine serum (FCS), 100 units/ml penicillin G, 100 μg/ml streptomycin, and 2 mM glutamine. 293T cells were propagated in Dulbecco's modified Eagle's medium (DMEM) supplemented with 10% FCS. $Bax^{-/-}Bak^{-/-}$ MEFs were grown in DMEM supplemented with 10% FCS, 250 μM L-asparagine, and 55 μM 2-mercaptoethanol. Bak or Bax was stably introduced into $Bax^{-/-}Bak^{-/-}$ double knockout MEFs by retroviral transduction. Beginning 24 h after $Bax^{-/-}Bak^{-/-}$ MEFs were infected with pBabe-puro(+) encoding wt human Bak or Bax, cells were selected in DMEM (10% FCS) with 2 μg/ml puromycin for 2 weeks. Stable clones were isolated using cloning rings, expanded, and analyzed for Bak expression by immunoblotting.

Mammalian Expression Plasmids and Transient Transfection—cDNAs encoding human Bim_{EL} (GenBank™ AF032457), Pumaα (GenBank™ NM_001127242), Noxa (GenBank™ NM_021127), and Bad (GenBank™ AF021792) were cloned into the Xho1 and BamH1 sites of pEGFP-C1 to yield constructs fused at their N termini to EGFP. Empty pEGFP-C1 served as a control. Plasmids encoding S peptide-tagged Bim_{EL}, Puma, Noxa, and Bad were constructed in pSPN (64) as described previously (68).

Log phase Jurkat cells or SKW 6.4 cells growing in antibiotic-free medium were transiently transfected with the indicated plasmid using a BTX 830 square wave electroporator delivering a single pulse at 240 mV for 10 ms. Cells were incubated for 24 h and analyzed for apoptosis using APC-coupled annexin V as previously described (68, 69).

Circular Dichroism (CD) Spectroscopy and α-Helicity Calculation—BH3 peptides or Bak as a positive control at 0.2 mg/ml were dissolved in HK buffer (20 mM HEPES, 150 mM NaCl (pH 7.0)) or 30% (v/v) 2,2,2-trifluoroethanol in HK buffer. CD spectra were collected at room temperature on a Jasco Spectropolarimeter 810 (Jasco, Inc., Easton, MD) in a 0.1-cm cuvette. Two sequential scans from 250 to 200 nm were recorded, and the background spectrum of the buffer only was subtracted. The k2d algorithm was utilized to calculate the α helical content of the protein.

Bak Complex Model Generation—The Puma·Bak and PumaIG·Bak complexes were generated from the coordinates of the Noxa·Bak complex (62, 70) in which Noxa was mutated to Puma and PumaIG, respectively, using MacPyMOL V1.5.0 (Schrödinger LLC, Portland, OR). The topology and coordinate files of the two complexes were generated by the tLeap module of the AmberTools12 program (University of California, San Francisco, CA). All His, Glu, Asp, and Cys residues of the two complexes were treated as HIP, GLU, ASP, and CYS, respectively, except that $His\text{-}164^{Bak}$ was treated as HID. The energy minimization of the complexes was performed by using the SANDER modules of the AMBER 11 program Version 11 with a dielectric constant of 1.0 and 200 cycles of steepest-descent minimization followed by 300 cycles of conjugate-gradient minimization using the ff12SB force field (71, 72). The Puma·Bak and PumaIG·Bak complexes were solvated by using the tLeap module with 6,514 and 6,577 TIP3P water molecules leading to a system of 22,548 and 22,736 atoms, respectively, using the distance parameter of 8.2 Å for the SolvateBox command.

Multiple Molecular Dynamics Simulations of the Bak Complexes—Each of the two solvated complexes was energy-minimized for 100 cycles of steepest-descent minimization followed by 900 cycles of conjugate-gradient minimization to remove close van der Waals contacts in the system, then heated from 0 to 300 K at a rate of 10 K/ps under constant temperature and volume, and finally simulated independently with a unique seed number for initial velocities at 300 K under constant temperature and pressure using the PMEMD module of the AMBER 11 program (University of California, San Francisco) with the ff12SB force field (71, 72). Ten 10-ns independent simulations

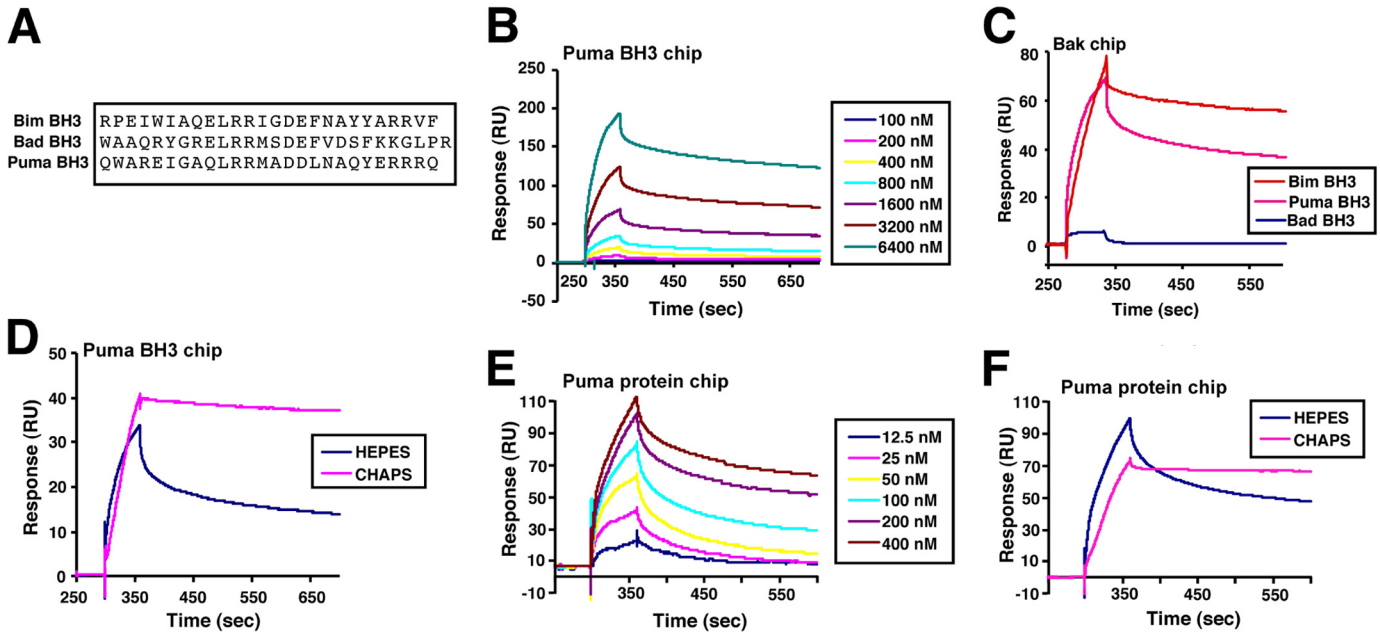

FIGURE 1. **Direct interaction of Puma BH3 peptide with Bak.** *A*, synthetic BH3 peptides used in this figure. *B*, SPR (relative units (*RU*)) observed when immobilized Puma BH3 peptide was exposed to increasing concentrations of purified BakΔTM. *C*, SPR of immobilized BakΔTM exposed to 2000 nM Bim BH3, Puma BH3, and Bad BH3. *D*, SPR of immobilized Puma BH3 exposed to 800 nM BakΔTM in buffer without or with 1% (w/v) CHAPS. *E*, SPR of immobilized Puma protein exposed to increasing concentrations of purified BakΔTM. *F*, SPR of immobilized Puma protein exposed to 200 nM BakΔTM in buffer without or with 1% (w/v) CHAPS. For additional primary data, see supplemental Figs. S1 and S3.

were performed for each of the two complexes. All simulations used (i) a dielectric constant of 1.0, (ii) the Berendsen coupling algorithm (73), (iii) a periodic boundary condition at a constant temperature of 300 K and a constant pressure of 1 atm with isotropic molecule-based scaling, (iv) the Particle Mesh Ewald method to calculate long-range electrostatic interactions (74), (v) a time step of 1.0 fs, (vi) the SHAKE-bond-length constraints applied to all the bonds involving the H atom, (vii) saving the image closest to the middle of the "primary box" to the restart and trajectory files, (viii) a formatted restart file, and (ix) default values of all other inputs of the PMEMD module. All simulations were performed on a cluster of Apple Mac Pros with 1200 Intel Xeon cores (2.4/2.9 GHz).

Bak Complex Model Analysis—Average conformations of the two complexes were obtained by using trajectories saved at 1-ps intervals during the last 2-ns period of the 10 10-ns simulations and the Ptraj module of the AmberTools12 program. These conformations were then energy-minimized using the SANDER module of the AMBER 11 program with a dielectric constant of 40.0 and 100 cycles of steepest-descent minimization followed by 100 cycles of conjugate-gradient minimization. The interaction energy between the BH3 domain and Bak in the energy-minimized average conformations was then calculated using an in-house program with a dielectric constant of 40.0 and a nonbonded cutoff of 50,000 Å.

Graphics—All figures were generated by using the MacPyMOL (V1.5.0) and Adobe Photoshop CS5 Extended Version 12.1 × 64 (Adobe Systems Incorporated, San Jose, CA) programs.

RESULTS AND DISCUSSION

Puma BH3 Binds Directly to Bak—Previous studies examining whether Puma is a direct activator have yielded contradictory results. Accordingly, using recently described approaches (62), we set out to determine whether the Puma BH3 domain (Fig. 1*A*) interacts directly with the multidomain pro-apoptotic protein Bak. The Bim BH3 domain (Fig. 1*A*), which has a similar degree of α-helical structure as assessed by circular dichroism spectroscopy (supplemental Fig. S1), served as a control.

When immobilized Puma BH3 peptide was exposed to increasing concentrations of purified, recombinant human Bak lacking the transmembrane domain (BakΔTM), increased binding was detected (Fig. 1*B*). Likewise, when immobilized BakΔTM was exposed to increasing concentrations of Puma BH3 peptide, increased binding was observed (supplemental Fig. S2*A*). Direct comparison of Bim BH3 and Puma BH3 binding to immobilized BakΔTM revealed that the Puma BH3 bound to Bak slightly more rapidly but also dissociated somewhat more rapidly (Fig. 1*C*). Consistent with these results, equilibrium dissociation constants (K_D values) of 260 ± 90 and 290 ± 130 nM were calculated for Bim BH3 and Puma BH3, respectively, binding to Bak (Table 1). In contrast, the Bad BH3 domain barely bound at all (Fig. 1*C* and Table 1). The addition of CHAPS to the binding assay (62) markedly diminished the

TABLE 1
Dissociation constants of Bak complexed with various BH3 peptides or Pumaα protein

BH3 peptides/ protein	Buffer[a]	
	HEPES	CHAPS
Bim BH3	260 ± 90 nM[b]	29 ± 5
Puma BH3	290 ± 130	26 ± 5
Bad BH3	9600 ± 1300	
Puma3E BH3	8000 ± 1050	
PumaIG BH3	190 ± 30	
Pumaα Protein	140 ± 40	17 ± 5

[a] From experiments performed in HEPES or CHAPS buffer, as illustrated in Figs. 1, 2, and 7 and supplemental Fig. S2, equilibrium dissociation (K_d) constants were calculated.
[b] Values are the mean ± S.D. of K_D values (nM) from three independent experiments.

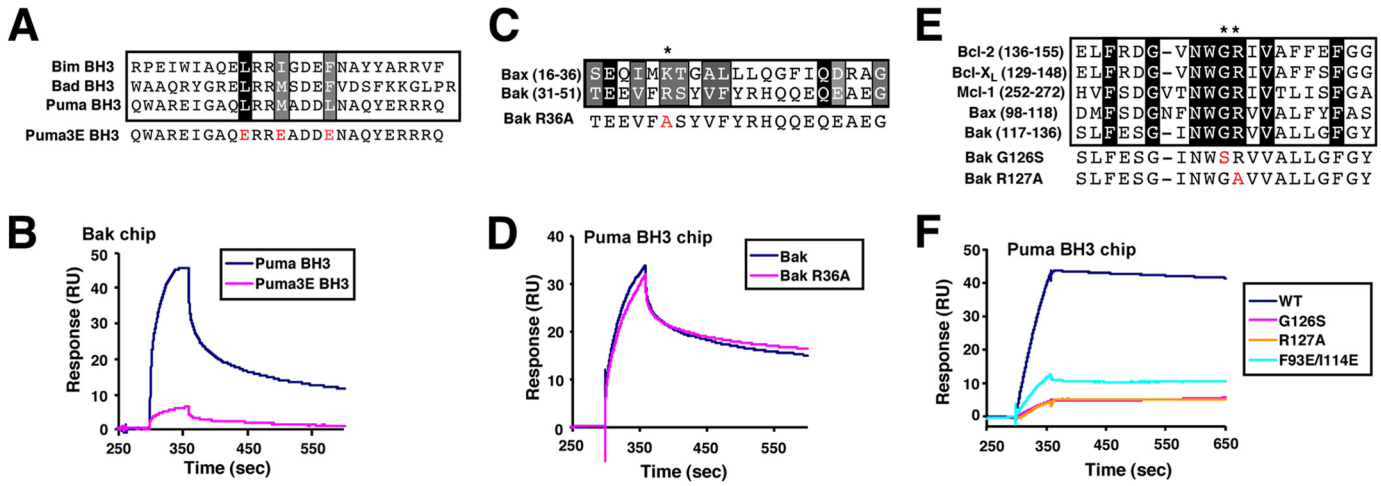

FIGURE 2. **Puma BH3 domain binds Bak in the canonical BH3-binding groove.** *A*, sequence alignment of synthesized human BH3 domains. Residues marked in *red* are three conserved hydrophobic residues mutated to Glu in the Puma3E BH3 peptide. *B*, SPR of immobilized BakΔTM exposed to 1000 nM Puma BH3 or Puma3E BH3. *C*, sequence alignment of Bax and Bak showing Bax Lys21 (*asterisk*) implicated in binding BH3 peptides to initiate oligomerization (75). *D*, SPR of immobilized Puma BH3 peptide exposed to 800 nM BakΔTM and BakΔTM R36A. *E*, sequence alignment of BH1 domains of human Bcl-2, Bcl-X_L, Mcl-1, Bax, and Bak. The conserved Gly and Arg residues in the BH3 binding groove that are critical for BH3 binding and are mutated in the indicated Bak mutants are shown in *red*. *F*, SPR of immobilized Puma BH3 exposed to 800 nM wild type BakΔTM, BakΔTM G126S, BakΔTM R127A, or BakΔTM F93E/I114E. *RU*, relative units.

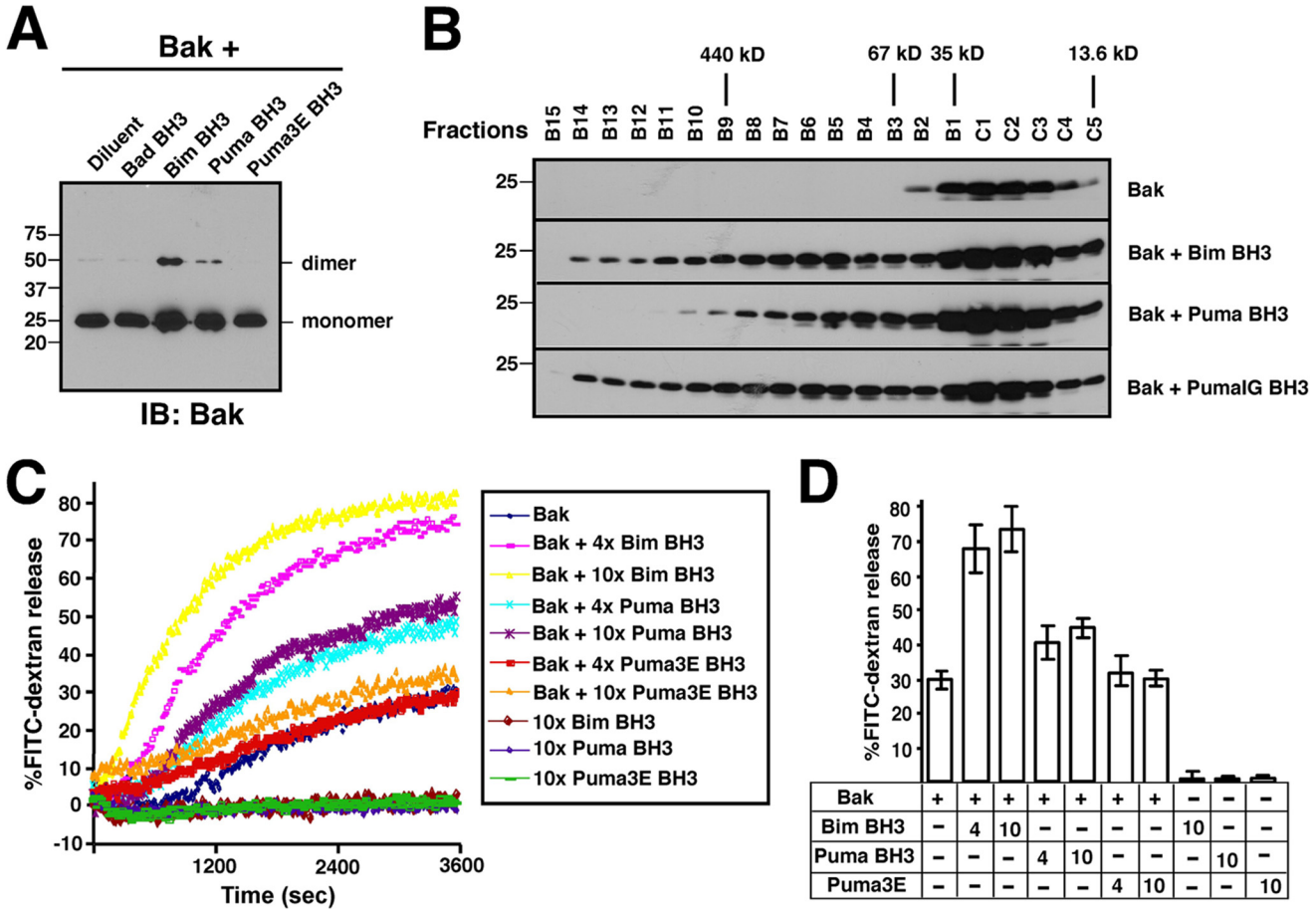

FIGURE 3. **The Puma BH3 domain can activate Bak.** *A*, 50 nM BakΔTM with or without the indicated BH3 peptide (200 nM) was incubated with liposomes composed of mitochondrial outer membrane lipids for 30 min, cross-linked with 100 μM BMH, subjected to SDS-PAGE, and analyzed by immunoblotting (*IB*). Locations of Bak monomer and dimer are shown. *B*, after BakΔTM without or with a 3-fold molar excess of the indicated peptide was incubated as indicated under "Experimental Procedures," samples were subjected to FPLC, and fractions were blotted for Bak. *Numbers* above column fractions indicate size markers separated on the same column. *C* and *D*, liposome release assay performed in the absence or presence of 50 nM BakΔTM and the indicated BH3 peptide at 200 nM (4×) or 500 nM (10×). A representative experiment (*C*) and summary of the percentage of FITC-dextran release (*D*) are shown. *Error bars*, mean ± S.D. of three independent experiments using different protein preparations. Additional release assays are summarized in supplemental Fig. S4.

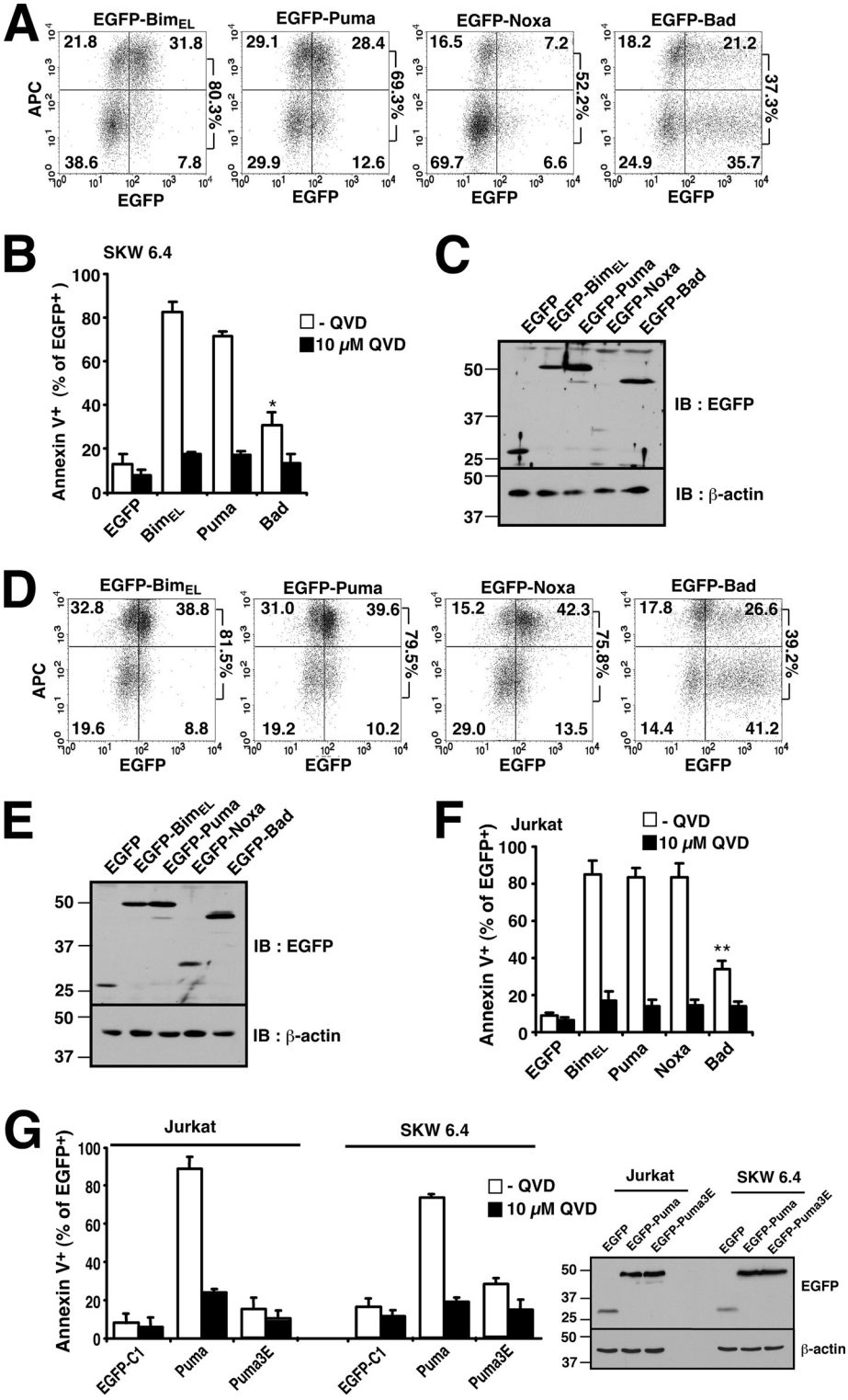

FIGURE 4. **Puma kills cell through its BH3 domain.** *A–F*, 24 h after SKW 6.4 cells (*A* and *B*) or Jurkat cells (*D* and *F*) were transfected with cDNA encoding EGFP or EGFP fused to Bim$_{EL}$, Pumaα, Noxa, or Bad in the presence or absence of 10 μM Q-VD-OPh (*QVD*), cells were stained with APC-annexin V and subjected to flow microfluorimetry. Representative experiments (*A* and *D*) and summarized results (*B* and *F*) indicate the percentage of EGFP$^+$ cells stained with APC-annexin V. *Numbers* in each quadrant represent the percentage of events in each category defined by the *cross bars*. *Numbers at the right of the dot plots* in this and subsequent figures indicate the ratio of events in the *upper right panel* to the sum of the *lower right and upper right*. *Error bars*, mean ± S.D. of three independent experiments. * in *B*, $p < 0.001$ *versus* EGFP-Bim$_{EL}$ and EBFP-Puma as analyzed by analysis of variance with post hoc *t* tests and Bonferroni correction. *F*, **, $p < 0.0005$ *versus* EGFP-Bim$_{EL}$, EGFP-Puma, or EGFP-Noxa using the same statistical analysis. *C* and *E*, whole cell lysates of transfected cells treated with 10 μM Q-VD-OPh were subjected to immunoblotting (*IB*). *G*, 24 h after Jurkat cells or SKW 6.4 cells were transfected with cDNA encoding EGFP, EGFP-Pumaα, or EGF-Pumaα L141E/M144E/L148E (EGFP-Pumaα 3E) in the presence or absence of 10 μM Q-VD-OPh, cells were stained with APC-annexin V. The percentage of EGFP$^+$ cells stained with APC-annexin V is indicated. *Inset*, whole cell lysates of cells treated with 10 μM Q-VD-OPh were subjected to immunoblotting. *Error bars*, mean ± S.D. of three independent experiments. Additional results are shown in supplemental Fig. S5.

dissociation rate (Fig. 1*D*), as was also seen with the Bim BH3 domain. Accordingly, the K_D values for Puma and Bim BH3 domains bound to Bak decreased to 26 ± 5 and 29 ± 5 nM, respectively, in the presence of 1% CHAPS (Table 1).

To rule out the possibility that binding was unique to Puma BH3 peptides and would not be seen with the Puma protein, we optimized codon usage in the human Pumaα cDNA (supplemental Fig. S3) for expression in *E. coli*. As was seen with the Puma BH3 domain peptide, Bak bound to the immobilized recombinant Pumaα (Fig. 1*E*) with a K_D of 140 ± 40 nM. Once again, the addition of CHAPS enhanced the affinity almost 10-fold (Fig. 1*F* and Table 1).

Puma BH3 Peptide Binds the Canonical BH3 Binding Groove of Bak—Examination of a Puma BH3 peptide in which the three conserved hydrophobic residues in the BH3 domain were changed to glutamate (Puma3E BH3, Fig. 2*A*) revealed diminished binding to Bak (Fig. 2*B* and supplemental Fig. S2), just as was previously observed for Noxa3E binding to Bak (62). These observations indicate that residues previously implicated in binding of Noxa to Bak are also important in binding of Puma to Bak.

Recent studies of BH3 peptide binding to Bax have yielded contradictory results, with the Bim BH3 peptide reportedly binding to a shallow groove near the Bax N terminus (75) and alternatively to the canonical BH3 binding groove vacated by the Bax α9 helix after a putative conformational change in Bax (63). To assess whether the Puma BH3 peptide was binding to a portion of Bak corresponding to the so-called "trigger" site on Bax, Arg-36 of Bak was mutated to Ala (Fig. 2*C*) to mimic the critical K21A mutation in Bax (75). This mutation had no effect on binding of Bak to immobilized Puma (Fig. 2*D*). In contrast, mutation of critical residues in the canonical BH3 binding groove of Bak (62) diminished the binding of Bak to immobilized Puma BH3 domain (Fig. 2, *E* and *F*). These included the Bak R127A mutation, which replaces the invariant Arg presence in the BH3 binding groove of all multidomain Bcl-2 family members (Fig. 2*E*), and the Bak G126S mutation, which replaces Gly-126 with a bulkier Ser residue that sterically hinders binding of BH3 domains (76). The marked inhibitory effect of these mutations (Fig. 2*F*) suggests that the Puma BH3 domain binds directly to the canonical BH3 binding groove of Bak and not an alternative site.

Puma BH3 Induces Bak Oligomerization and Bak-mediated Membrane Permeabilization—Our previous results indicated that binding of BH3-only proteins to the BH3 binding groove of Bak is the first step in Bak oligomerization (62). To determine whether the Puma BH3 domain also induced Bak oligomerization, Bak was incubated with liposomes composed of mitochondrial outer membrane lipids (23, 66) in the absence or presence of the Puma BH3 domain peptide, cross-linked with BMH, subjected to SDS-PAGE, and analyzed for dimers by immunoblotting. Positive and negative controls, respectively, were the Bim BH3 peptide, which is known to activate Bak, and the Bad BH3 peptide, which is not able to activate Bak (62). As indicated in Fig. 3*A*, the Puma BH3 domain, like the Bim BH3 domain, induced Bak oligomerization. In contrast, the Puma3E BH3 mutant, which is unable to bind Bak (Fig. 2*B*), did not induce Bak oligomerization.

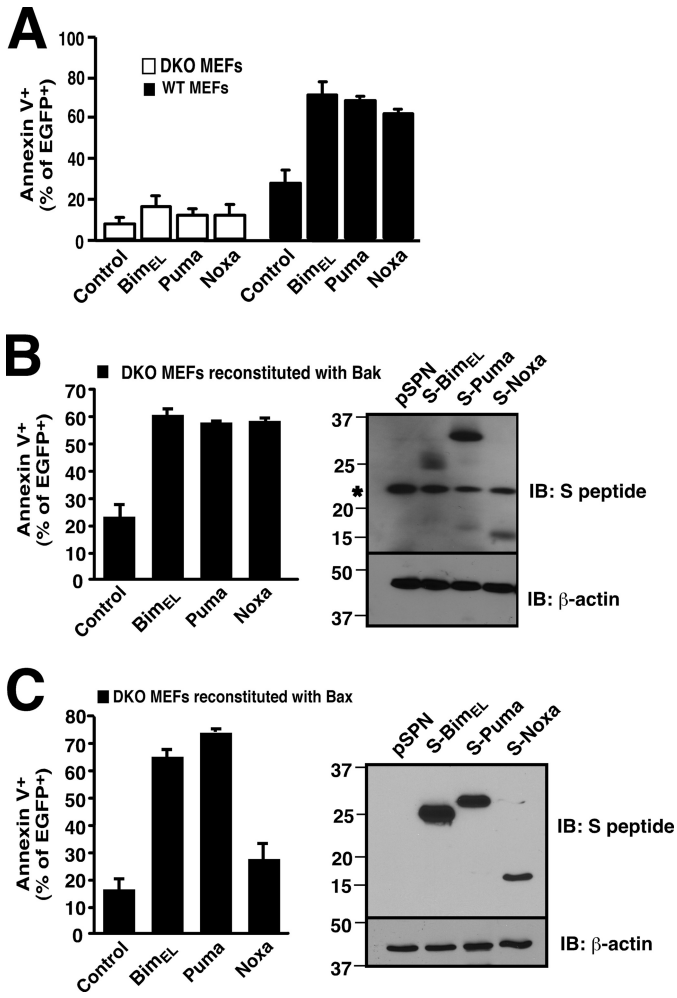

FIGURE 5. **Dependence of BH3 only protein-induced apoptosis in MEFs on Bax or Bak.** *A*, 24 h after Bak$^{-/-}$/Bax$^{-/-}$ double knockout (*DKO*) MEFs and wild type MEFs were transfected with plasmid encoding S peptide-tagged Bim$_{EL}$, Pumaα, Noxa, or empty vector together with plasmid encoding EGFP-Histone H2B (8:1 ratio), cells were stained with APC-annexin V and analyzed by flow microfluorimetry. The percentage of EGFP$^+$ cells stained with annexin V is shown. *B* and *C*, 24 h after Bak$^{-/-}$/Bax$^{-/-}$ MEFs reconstituted with wild type Bak (*B*) or Bax (*C*) were transfected cDNA encoding S peptide-tagged Bim$_{EL}$, Pumaα, or Noxa, cells were collected and stained with APC-annexin V. The percentage of EGFP$^+$ cells stained with annexin V is shown. *Right panels* in *B* and *C*, after transfection cells were incubated for 24 h in the presence of 5 μM Q-VD-OPh. Whole cell lysates were subjected to SDS-PAGE and immunoblotting (*IB*) with antibodies to the indicated antigens. *, nonspecific band.

In further experiments Bak oligomerization was also examined by FPLC. In these experiments, the Bim BH3 peptide induced a shift of Bak from monomer to higher order oligomers (Fig. 3*B*). Likewise, the Puma BH3 domain induced oligomerization, albeit less extensive than that seen with the Bim BH3 domain (*cf. two middle panels* in Fig. 3*B*).

To assess whether the oligomerized Bak was biologically active, liposome permeabilization was assessed. The Puma BH3 peptide, like the Bim or Bak BH3 domains, increased Bak-mediated release of fluoresceinated dextran from the liposomes (Fig. 3, *C* and *D*, and supplemental Fig. S4). In contrast, like the Bad BH3 domain, the Puma3E BH3 did not (Fig. 3, *C* and *D*, and supplemental Fig. S4). Importantly, the Puma or Bim BH3 peptides by themselves had no effect on liposome permeability (Fig. 3, *C* and *D*). Collectively, the results in Figs. 2 and 3

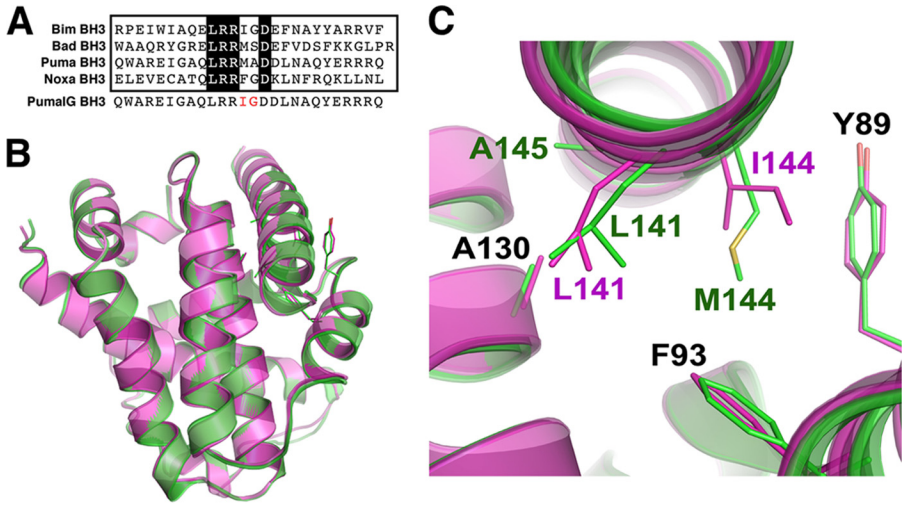

FIGURE 6. **Rationale for examining PumaIG.** *A*, sequence alignment of synthesized human BH3 domains. The indicated Met-144 and Ala-145 residues in the Puma BH3 were mutated to Ile and Gly (shown in *red*) to generate a more potent activator peptide "PumaIG BH3." *B* and *C*, structural analysis of Puma BH3 (wild type and M144I/A145G mutant) in the Bak BH3 binding groove. Wild type Puma is shown in *green*, and PumaIG BH3 is in *pink*.

indicate that binding of the Puma BH3 domain to the Bak BH3 binding groove is sufficient to induce Bak oligomerization and activation.

Direct Puma·Bak Interactions Are Sufficient for Puma-mediated Killing—Consistent with previous results indicating that transfection of Pumaα is sufficient to induce apoptosis in colon cancer cells and mouse embryonic fibroblasts (27, 52), we observed that EGFP-Pumaα, like EGFP-Bim$_{EL}$ or EGFP-Noxa, is able to induce apoptosis in SKW6.4 cells (Fig. 4, *A–C*, and supplemental Fig. S5). In contrast, EGFP-Bad induced much less apoptosis. Likewise, in Jurkat cells, where virtually all mitochondrial apoptosis is Bak-dependent (78, 79), EGFP-Pumaα was readily able to induce apoptosis, as was EGFP-Bim$_{EL}$ or EGFP-Noxa but not EGFP-Bad (Fig. 4, *D–F*). Importantly, the ability of EGFP-Pumaα to induce apoptosis in all of these cellular contexts was markedly diminished by the L141E/M144E/L148E mutation in its BH3 domain (Fig. 4*G* and supplemental Fig. S5).

In further experiments, the ability of Pumaα to induce apoptosis was compared in wild type MEFs, *Bax*$^{-/-}$/*Bak*$^{-/-}$ double knock-out MEFs and double knock-out MEFs reconstituted with Bak or Bax. Results of this analysis demonstrated that Pumaα, like Bim$_{EL}$ and Noxa, was unable to induce apoptosis in the absence of Bax and Bak (Fig. 5*A*). When MEFs were reconstituted with either Bak (Fig. 5*B*) or Bax (Fig. 5*C*), Pumaα was able to induce apoptosis, consistent with a recent report suggesting that Puma can also directly activate Bax (58). Bim$_{EL}$ likewise induced apoptosis in MEFs reconstituted with either Bax or Bak, whereas Noxa selectively induced apoptosis only in MEFs reconstituted with Bak (Fig. 5, *B* and *C*).

A Puma BH3 Mutant That Enhances Puma Function—Close examination indicated that the Puma BH3 peptide bound Bak slightly less tightly (Fig. 1*C* and Table 1), oligomerized Bak somewhat less effectively (Fig. 3, *A* and *B*), and permeabilized liposomes less efficiently (Fig. 3, *C* and *D*) than the corresponding Bim peptide. Likewise, EGFP-Pumaα killed SKW6.4 cells less effectively than EGFP-Bim$_{EL}$ (Fig. 4*B*). Comparison of the Puma BH3 peptide to other direct activator BH3 domains indicated that the Ile-Gly dipeptide found between the conserved Arg-154 and Asp-157 in Bim$_{EL}$ is replaced by the bulkier Met-Ala in Puma (Fig. 6*A*). Molecular dynamics simulations predicted that mutation of Met-Ala to Ile-Gly would make the Puma mutant bind ~0.5 Å deeper in the Bak BH3 binding groove than the wild type (Fig. 6, *B* and *C*), which would also decrease the intermolecular interaction energy (Table 2). In addition, mutation of Met to Ile would allow more spin of the phenyl ring of Phe-93 in Bak, as is evident from the more contracted ring of Phe-93 in the time-average structure of PumaIG·Bak than that in the wild type complex shown in Fig. 6*C*. Collectively, these observations predict an increased affinity of the PumaIG·Bak complex that is due to improvements from enthalpy and configurational entropy (77).

To test these predictions, we compared the Puma and PumaIG BH3 peptides in the assays shown in Figs. 1–3. Compared with the wild type sequence, the degree of α-helicity of the peptide was unchanged (supplemental Fig. S6). Nonetheless, PumaIG BH3 bound immobilized Bak more tightly (Fig. 7*A*), oligomerized Bak more effectively (Figs. 3*B* and 7*B*), and induced greater Bak-mediated permeabilization of liposomes composed of mitochondrial outer membrane lipids (Fig. 7, *C* and *D*). Similar effects on Bak-mediated permeabilization were also observed using purified mitochondria (Fig. 7*E*). Consistent with these results, Pumaα with the corresponding IG mutation in its BH3 domain also killed SKW6.4 cells

TABLE 2
Calculated intermolecular interaction energies of BH3 domains with Bak or mMcl-1

The intermolecular interaction energies (E) of $A_{26}K$·Bak (used as a negative control), *m*NoxaA·Mcl-1 and Puma·Mcl-1 were reported in Dai *et al.* (62).

Complex	E_{total}	E_{vdw}	E_{ele}
	kcal/mol	*kcal/mol*	*kcal/mol*
PumaIG·Bak	−134.4	−128.4	−6.0
Puma·Bak	−125.5	−119.3	−6.2
Noxa·Bak	−132.0	−126.9	−4.8
$A_{26}K$·Bak	−110.4	−109.8	−0.4
*m*Noxa]*m*Mcl-1	−176.2	−172.7	−3.1
*m*Puma·*m*Mcl-1	−152.4	−149.0	−3.0

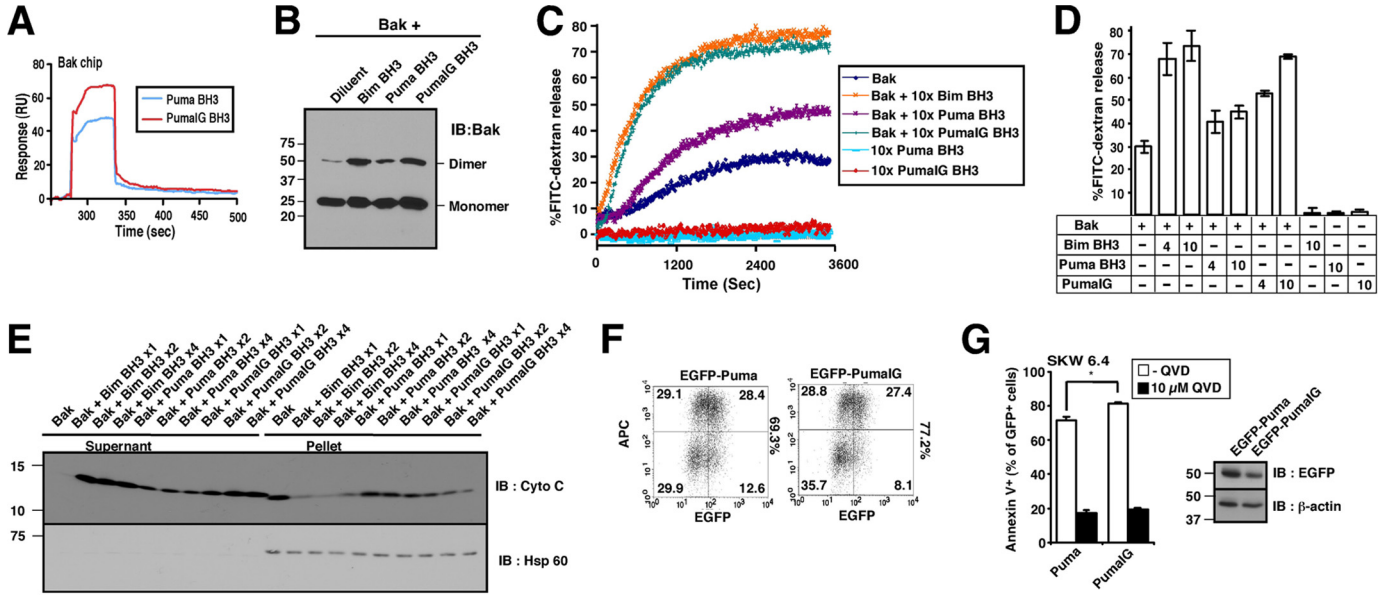

FIGURE 7. **PumaIG BH3 induces more Bak activation.** *A*, SPR (relative units) of 2 μM Puma BH3 or PumaIG BH3 binding to immobilized BakΔTM. *B*, liposomes were incubated for 30 min with 50 nM BakΔTM without or with 200 nM Bim BH3, Puma BH3, or PumaIG BH3, cross-linked with 100 μM BMH, subjected to SDS-PAGE, and analyzed by immunoblotting (*IB*). *RU*, relative units. *C* and *D*, liposome release assay performed in the presence of 50 nM Bak in the absence or presence of 200 nM (4×) or 500 nM (10×) Bim BH3, Puma BH3, or PumaIG BH3. A representative experiment (*D*) and summary of the percentage of FITC-dextran release from liposomes (*E*) from three independent experiments are shown. *E*, mitochondria from $Bax^{-/-}Bak^{-/-}$ MEFs were incubated with purified BakΔTM and the indicated BH3 peptide at 23 °C for 2 h, sedimented, and washed. The supernatant and pellet were subjected to SDS-PAGE and immunoblotting. *F* and *G*, 24 h after SKW 6.4 cells were transfected with EGFP-Puma or EGFP-PumaIG, cells were stained with APC-annexin V and analyzed by flow microfluorimetry. A representative experiment (*F*) and summarized results (*G*) indicates the percentage of $EGFP^+$ cells stained with APC-annexin V. *, $p = 0.012$ by 2-sided *t* test. *Inset* in *G*, after transfected cells were treated with 10 μM QVD for 24 h, whole cell lysates were subjected to immunoblotting.

slightly more effectively despite somewhat lower overall expression (Fig. 7, *F* and *G*).

Conclusions—Previous studies have reached conflicting conclusions regarding the role of Puma in activating Bax and/or Bak. Even in those studies where a direct interaction between Puma and Bax or Bak was suggested, the strength of the interaction was not assessed, and domains responsible for the interaction were not conclusively identified. Recent studies have demonstrated that direct activator BH3 proteins can be distinguished from sensitizers based on (i) their ability to directly bind to Bak and/or Bax by surface plasmon resonance analysis, (ii) their ability to oligomerize Bax or Bak *in vitro* in the absence of other proteins, and (iii) their ability to induce Bax- or Bak-dependent permeabilization of liposomes composed of mitochondrial outer membrane lipids. Our results demonstrate that under various conditions the Puma BH3 domain binds Bak almost as tightly as the BH3 domain of Bim, a known direct activator. In contrast to results published examining binding of Puma BH3 derivatives to Bax while this work was under review (58), the binding of the Puma BH3 to Bak was observed without introduction of hydrophobic moieties that constrain the conformation of the Puma BH3 domain. Moreover, full-length Pumaα protein retains the ability to bind Bak. This binding involves the canonical BH3 binding pocket of Bak rather than a trigger site on the opposite side of the protein. Mutations that diminish (Puma3E BH3) or enhance (PumaIG BH3) the Puma BH3 domain·Bak BH3 binding groove interaction result in a corresponding change in the oligomerization of Bak, the induction of Bak-mediated liposome or mitochondrial permeabilization, and Puma-induced killing in intact cells. Accordingly, it appears that Puma displays all of the properties of a direct Bak activator.

Acknowledgments—We gratefully acknowledge kind gifts of plasmids from Qian Liu and Kalle Gehrig, the editorial assistance of Deb Strauss, and helpful discussions with Greg Gores, Andreas Strasser, and members of the Kaufmann laboratory.

REFERENCES

1. Wyllie, A. H., Kerr, J. F., and Currie, A. R. (1980) Cell death. The significance of apoptosis. *Int. Rev. Cytol.* **68,** 251–306
2. Thompson, C. B. (1995) Apoptosis in the pathogenesis and treatment of disease. *Science* **267,** 1456–1462
3. Adjei, P. N., Kaufmann, S. H., Leung, W. Y., Mao, F., and Gores, G. J. (1996) Selective induction of apoptosis in Hep 3B cells by topoisomerase I inhibitors. Evidence for a protease-dependent pathway that does not activate CPP32. *J Clin. Invest.* **98,** 2588–2596
4. Kroemer, G., and Martin, S. J. (2005) Caspase-independent cell death. *Nat. Med.* **11,** 725–730
5. Tait, S. W., and Green, D. R. (2008) Caspase-independent cell death. Leaving the set without the final cut. *Oncogene* **27,** 6452–6461
6. Earnshaw, W. C., Martins, L. M., and Kaufmann, S. H. (1999) Mammalian caspases. Structure, Activation, Substrates, and functions during apoptosis. *Annu. Rev. Biochem.* **68,** 383–424
7. Creagh, E. M., and Martin, S. J. (2001) Caspases. Cellular demolition experts. *Biochem. Soc. Trans.* **29,** 696–702
8. Walczak, H., and Krammer, P. H. (2000) The CD95 (APO-1/Fas) and the TRAIL (APO-2L) apoptosis systems. *Exp. Cell Res.* **256,** 58–66
9. Debatin, K. M., and Krammer, P. H. (2004) Death receptors in chemotherapy and cancer. *Oncogene* **23,** 2950–2966
10. Schütze, S., Tchikov, V., and Schneider-Brachert, W. (2008) Regulation of TNFR1 and CD95 signalling by receptor compartmentalization. *Nat. Rev. Mol. Cell Biol.* **9,** 655–662

11. Johnstone, R. W., Frew, A. J., and Smyth, M. J. (2008) The TRAIL apoptotic pathway in cancer onset, progression, and therapy. *Nat. Rev. Cancer* **8,** 782–798
12. Abdulghani, J., and El-Deiry, W. S. (2010) TRAIL receptor signaling and therapeutics. *Expert. Opin. Ther. Targets* **14,** 1091–1108
13. Afonina, I. S., Cullen, S. P., and Martin, S. J. (2010) Cytotoxic and non-cytotoxic roles of the CTL/NK protease granzyme B. *Immunol. Rev.* **235,** 105–116
14. Ewen, C. L., Kane, K. P., and Bleackley, R. C. (2012) A quarter century of granzymes. *Cell Death Differ.* **19,** 28–35
15. Jiang, X., and Wang, X. (2004) Cytochrome *c*-mediated apoptosis. *Annu. Rev. Biochem.* **73,** 87–106
16. Taylor, R. C., Cullen, S. P., and Martin, S. J. (2008) Apoptosis. Controlled demolition at the cellular level. *Nat. Rev. Mol. Cell Biol.* **9,** 231–241
17. Tait, S. W., and Green, D. R. (2010) Mitochondria and cell death. Outer membrane permeabilization and beyond. *Nat. Rev. Mol. Cell Biol.* **11,** 621–632
18. Strasser, A., Cory, S., and Adams, J. M. (2011) Deciphering the rules of programmed cell death to improve therapy of cancer and other diseases. *EMBO J.* **30,** 3667–3683
19. Letai, A. G. (2008) Diagnosing and exploiting cancer's addiction to blocks in apoptosis. *Nat. Rev. Cancer* **8,** 121–132
20. Chipuk, J. E., Moldoveanu, T., Llambi, F., Parsons, M. J., and Green, D. R. (2010) The BCL-2 family reunion. *Mol. Cell* **37,** 299–310
21. Letai, A., Bassik, M. C., Walensky, L. D., Sorcinelli, M. D., Weiler, S., and Korsmeyer, S. J. (2002) Distinct BH3 domains either sensitize or activate mitochondrial apoptosis, serving as prototype cancer therapeutics. *Cancer Cell* **2,** 183–192
22. Kuwana, T., Mackey, M. R., Perkins, G., Ellisman, M. H., Latterich, M., Schneiter, R., Green, D. R., and Newmeyer, D. D. (2002) Bid, Bax, and lipids cooperate to form supramolecular openings in the outer mitochondrial membrane. *Cell* **111,** 331–342
23. Kuwana, T., Bouchier-Hayes, L., Chipuk, J. E., Bonzon, C., Sullivan, B. A., Green, D. R., and Newmeyer, D. D. (2005) BH3 Domains of BH3-only proteins differentially regulate Bax-mediated mitochondrial membrane permeabilization both directly and indirectly. *Mol. Cell* **17,** 525–535
24. Fadeel, B., Zhivotovsky, B., and Orrenius, S. (1999) All along the watchtower. On the regulation of apoptosis regulators. *FASEB J.* **13,** 1647–1657
25. Chipuk, J. E., and Green, D. R. (2008) How do BCL-2 proteins induce mitochondrial outer membrane permeabilization? *Trends Cell Biol.* **18,** 157–164
26. Mérino, D., Giam, M., Hughes, P. D., Siggs, O. M., Heger, K., O'Reilly, L. A., Adams, J. M., Strasser, A., Lee, E. F., Fairlie, W. D., and Bouillet, P. (2009) The role of BH3-only protein Bim extends beyond inhibiting Bcl-2-like prosurvival proteins. *J. Cell Biol.* **186,** 355–362
27. Yu, J., Zhang, L., Hwang, P. M., Kinzler, K. W., and Vogelstein, B. (2001) PUMA induces the rapid apoptosis of colorectal cancer cells. *Mol. Cell* **7,** 673–682
28. Nakano, K., and Vousden, K. H. (2001) PUMA, a novel proapoptotic gene, is induced by p53. *Mol. Cell* **7,** 683–694
29. Villunger, A., Michalak, E. M., Coultas, L., Müllauer, F., Böck, G., Ausserlechner, M. J., Adams, J. M., and Strasser, A. (2003) p53- and drug-induced apoptotic responses mediated by BH3-only proteins puma and noxa. *Science* **302,** 1036–1038
30. Jeffers, J. R., Parganas, E., Lee, Y., Yang, C., Wang, J., Brennan, J., MacLean, K. H., Han, J., Chittenden, T., Ihle, J. N., McKinnon, P. J., Cleveland, J. L., and Zambetti, G. P. (2003) Puma is an essential mediator of p53-dependent and -independent apoptotic pathways. *Cancer Cell* **4,** 321–328
31. Yu, J., Wang, Z., Kinzler, K. W., Vogelstein, B., and Zhang, L. (2003) PUMA mediates the apoptotic response to p53 in colorectal cancer cells. *Proc. Natl. Acad. Sci. U.S.A.* **100,** 1931–1936
32. Erlacher, M., Michalak, E. M., Kelly, P. N., Labi, V., Niederegger, H., Coultas, L., Adams, J. M., Strasser, A., and Villunger, A. (2005) BH3-only proteins Puma and Bim are rate-limiting for γ-radiation- and glucocorticoid-induced apoptosis of lymphoid cells in vivo. *Blood* **106,** 4131–4138
33. Erlacher, M., Labi, V., Manzl, C., Böck, G., Tzankov, A., Häcker, G., Michalak, E., Strasser, A., and Villunger, A. (2006) Puma cooperates with Bim, the rate-limiting BH3-only protein in cell death during lymphocyte development, in apoptosis induction. *J. Exp. Med.* **203,** 2939–2951
34. Michalak, E. M., Villunger, A., Adams, J. M., and Strasser, A. (2008) In several cell types tumour suppressor p53 induces apoptosis largely via Puma but Noxa can contribute. *Cell Death Differ* **15,** 1019–1029
35. Qiu, W., Carson-Walter, E. B., Liu, H., Epperly, M., Greenberger, J. S., Zambetti, G. P., Zhang, L., and Yu, J. (2008) PUMA regulates intestinal progenitor cell radiosensitivity and gastrointestinal syndrome. *Cell Stem Cell* **2,** 576–583
36. Happo, L., Cragg, M. S., Phipson, B., Haga, J. M., Jansen, E. S., Herold, M. J., Dewson, G., Michalak, E. M., Vandenberg, C. J., Smyth, G. K., Strasser, A., Cory, S., and Scott, C. L. (2010) Maximal killing of lymphoma cells by DNA damage-inducing therapy requires not only the p53 targets Puma and Noxa, but also Bim. *Blood* **116,** 5256–5267
37. Yu, H., Shen, H., Yuan, Y., XuFeng, R., Hu, X., Garrison, S. P., Zhang, L., Yu, J., Zambetti, G. P., and Cheng, T. (2010) Deletion of Puma protects hematopoietic stem cells and confers long-term survival in response to high-dose γ-irradiation. *Blood* **115,** 3472–3480
38. Kerr, J. B., Hutt, K. J., Michalak, E. M., Cook, M., Vandenberg, C. J., Liew, S. H., Bouillet, P., Mills, A., Scott, C. L., Findlay, J. K., and Strasser, A. (2012) DNA damage-induced primordial follicle oocyte apoptosis and loss of fertility require TAp63-mediated induction of Puma and Noxa. *Mol. Cell* **48,** 343–352
39. Ekert, P. G., Jabbour, A. M., Manoharan, A., Heraud, J. E., Yu, J., Pakusch, M., Michalak, E. M., Kelly, P. N., Callus, B., Kiefer, T., Verhagen, A., Silke, J., Strasser, A., Borner, C., and Vaux, D. L. (2006) Cell death provoked by loss of interleukin-3 signaling is independent of Bad, Bim, and PI3 kinase but depends in part on Puma. *Blood* **108,** 1461–1468
40. Ekoff, M., Kaufmann, T., Engström, M., Motoyama, N., Villunger, A., Jönsson, J. I., Strasser, A., and Nilsson, G. (2007) The BH3-only protein Puma plays an essential role in cytokine deprivation induced apoptosis of mast cells. *Blood* **110,** 3209–3217
41. Jabbour, A. M., Daunt, C. P., Green, B. D., Vogel, S., Gordon, L., Lee, R. S., Silke, N., Pearson, R. B., Vandenberg, C. J., Kelly, P. N., Nutt, S. L., Strasser, A., Borner, C., and Ekert, P. G. (2010) Myeloid progenitor cells lacking p53 exhibit delayed up-regulation of Puma and prolonged survival after cytokine deprivation. *Blood* **115,** 344–352
42. Garrison, S. P., Jeffers, J. R., Yang, C., Nilsson, J. A., Hall, M. A., Rehg, J. E., Yue, W., Yu, J., Zhang, L., Onciu, M., Sample, J. T., Cleveland, J. L., and Zambetti, G. P. (2008) Selection against PUMA gene expression in Myc-driven B-cell lymphomagenesis. *Mol. Cell Biol.* **28,** 5391–5402
43. Michalak, E. M., Jansen, E. S., Happo, L., Cragg, M. S., Tai, L., Smyth, G. K., Strasser, A., Adams, J. M., and Scott, C. L. (2009) Puma and to a lesser extent Noxa are suppressors of Myc-induced lymphomagenesis. *Cell Death Differ.* **16,** 684–696
44. Bean, G. R., Ganesan, Y. T., Dong, Y., Takeda, S., Liu, H., Chan, P. M., Huang, Y., Chodosh, L. A., Zambetti, G. P., Hsieh, J. J., and Cheng, E. H. (2013) PUMA and BIM are required for oncogene inactivation-induced apoptosis. *Sci. Signal.* **6,** ra20
45. Concannon, C. G., Koehler, B. F., Reimertz, C., Murphy, B. M., Bonner, C., Thurow, N., Ward, M. W., Villunger, A., Strasser, A., Kögel, D., and Prehn, J. H. (2007) Apoptosis induced by proteasome inhibition in cancer cells. Predominant role of the p53/PUMA pathway. *Oncogene* **26,** 1681–1692
46. Steckley, D., Karajgikar, M., Dale, L. B., Fuerth, B., Swan, P., Drummond-Main, C., Poulter, M. O., Ferguson, S. S., Strasser, A., and Cregan, S. P. (2007) Puma is a dominant regulator of oxidative stress induced Bax activation and neuronal apoptosis. *J. Neurosci.* **27,** 12989–12999
47. Ghosh, A. P., Walls, K. C., Klocke, B. J., Toms, R., Strasser, A., and Roth, K. A. (2009) The proapoptotic BH3-only, Bcl-2 family member, Puma is critical for acute ethanol-induced neuronal apoptosis. *J. Neuropathol. Exp. Neurol.* **68,** 747–756
48. Bernstein, A. I., Garrison, S. P., Zambetti, G. P., and O'Malley, K. L. (2011) 6-OHDA generated ROS induces DNA damage and p53- and PUMA-dependent cell death. *Mol. Neurodegener.* **6,** 2
49. Fischer, S. F., Belz, G. T., and Strasser, A. (2008) BH3-only protein Puma contributes to death of antigen-specific T cells during shutdown of an immune response to acute viral infection. *Proc. Natl. Acad. Sci. U.S.A.* **105,** 3035–3040
50. Clybouw, C., Fischer, S., Auffredou, M. T., Hugues, P., Alexia, C., Bouillet,

P., Raphael, M., Leca, G., Strasser, A., Tarlinton, D. M., and Vazquez, A. (2011) Regulation of memory B-cell survival by the BH3-only protein Puma. *Blood* **118,** 4120–4128
51. Gray, D. H., Kupresanin, F., Berzins, S. P., Herold, M. J., O'Reilly, L. A., Bouillet, P., and Strasser, A. (2012) The BH3-only proteins Bim and Puma cooperate to impose deletional tolerance of organ-specific antigens. *Immunity* **37,** 451–462
52. Ren, D., Tu, H. C., Kim, H., Wang, G. X., Bean, G. R., Takeuchi, O., Jeffers, J. R., Zambetti, G. P., Hsieh, J. J., and Cheng, E. H. (2010) BID, BIM, and PUMA are essential for activation of the BAX- and BAK-dependent cell death program. *Science* **330,** 1390–1393
53. Jabbour, A. M., Heraud, J. E., Daunt, C. P., Kaufmann, T., Sandow, J., O'Reilly, L. A., Callus, B. A., Lopez, A., Strasser, A., Vaux, D. L., and Ekert, P. G. (2009) Puma indirectly activates Bax to cause apoptosis in the absence of Bid or Bim. *Cell Death Differ.* **16,** 555–563
54. Chipuk, J. E., and Green, D. R. (2009) PUMA cooperates with direct activator proteins to promote mitochondrial outer membrane permeabilization and apoptosis. *Cell Cycle* **8,** 2692–2696
55. Follis, A. V., Chipuk, J. E., Fisher, J. C., Yun, M. K., Grace, C. R., Nourse, A., Baran, K., Ou, L., Min, L., White, S. W., Green, D. R., and Kriwacki, R. W. (2013) PUMA binding induces partial unfolding within BCL-xL to disrupt p53 binding and promote apoptosis. *Nat. Chem. Biol.* **9,** 163–168
56. Gallenne, T., Gautier, F., Oliver, L., Hervouet, E., Noël, B., Hickman, J. A., Geneste, O., Cartron, P. F., Vallette, F. M., Manon, S., and Juin, P. (2009) Bax activation by the BH3-only protein Puma promotes cell dependence on antiapoptotic Bcl-2 family members. *J. Cell Biol.* **185,** 279–290
57. Kim, H., Tu, H. C., Ren, D., Takeuchi, O., Jeffers, J. R., Zambetti, G. P., Hsieh, J. J., and Cheng, E. H. (2009) Stepwise activation of BAX and BAK by tBID, BIM, and PUMA initiates mitochondrial apoptosis. *Mol. Cell* **36,** 487–499
58. Edwards, A. L., Gavathiotis, E., LaBelle, J. L., Braun, C. R., Opoku-Nsiah, K. A., Bird, G. H., and Walensky, L. D. (2013) Multimodal interaction with BCL-2 family proteins underlies the proapoptotic activity of PUMA BH3. *Chem. Biol.* **20,** 888–902
59. Zhang, Y., Xing, D., and Liu, L. (2009) PUMA promotes Bax translocation by both directly interacting with Bax and by competitive binding to Bcl-X L during UV-induced apoptosis. *Mol. Biol. Cell* **20,** 3077–3087
60. Vela, L., Gonzalo, O., Naval, J., and Marzo, I. (2013) Direct interaction of Bax and Bak proteins with Bcl-2 homology domain 3 (BH3)-only proteins in living cells revealed by fluorescence complementation. *J. Biol. Chem.* **288,** 4935–4946
61. Du, H., Wolf, J., Schafer, B., Moldoveanu, T., Chipuk, J. E., and Kuwana, T. (2011) BH3 domains other than Bim and Bid can directly activate Bax/Bak. *J. Biol. Chem.* **286,** 491–501
62. Dai, H., Smith, A., Meng, X. W., Schneider, P. A., Pang, Y.-P., and Kaufmann, S. H. (2011) Transient binding of an activator BH3 domain to the Bak BH3-binding groove initiates Bak oligomerization. *J. Cell Biol.* **194,** 39–48
63. Czabotar, P. E., Westphal, D., Dewson, G., Ma, S., Hockings, C., Fairlie, W. D., Lee, E. F., Yao, S., Robin, A. Y., Smith, B. J., Huang, D. C., Kluck, R. M., Adams, J. M., and Colman, P. M. (2013) Bax crystal structures reveal how BH3 domains activate Bax and nucleate its oligomerization to induce apoptosis. *Cell* **152,** 519–531
64. Hackbarth, J. S., Lee, S.-H., Meng, X. W., Vroman, B. T., Kaufmann, S. H., and Karnitz, L. M. (2004) S-peptide epitope tagging for protein purification, expression monitoring and localization in mammalian cells. *BioTechniques* **37,** 835–839
65. Moldoveanu, T., Liu, Q., Tocilj, A., Watson, M., Shore, G., and Gehring, K. (2006) The X-ray structure of a BAK homodimer reveals an inhibitory zinc binding site. *Mol. Cell* **24,** 677–688
66. Oh, K. J., Singh, P., Lee, K., Foss, K., Lee, S., Park, M., Lee, S., Aluvila, S., Park, M., Singh, P., Kim, R. S., Symersky, J., and Walters, D. E. (2010) Conformational changes in BAK, a pore-forming proapoptotic Bcl-2 family member, upon membrane insertion and direct evidence for the existence of BH3-BH3 contact interface in BAK homo-oligomers. *J. Biol. Chem.* **285,** 28924–28937
67. Goping, I. S., Gross, A., Lavoie, J. N., Nguyen, M., Jemmerson, R., Roth, K., Korsmeyer, S. J., and Shore, G. C. (1998) Regulated targeting of BAX to mitochondria. *J. Cell Biol.* **143,** 207–215
68. Meng, X. W., Lee, S. H., Dai, H., Loegering, D., Yu, C., Flatten, K., Schneider, P., Dai, N. T., Kumar, S. K., Smith, B. D., Karp, J. E., Adjei, A. A., and Kaufmann, S. H. (2007) Mcl-1 as a buffer for proapoptotic Bcl-2 family members during TRAIL-induced apoptosis. A mechanistic basis for sorafenib (Bay 43–9006)-induced TRAIL sensitization. *J. Biol. Chem.* **282,** 29831–29846
69. Mesa, R. A., Loegering, D., Powell, H. L., Flatten, K., Arlander, S. J., Dai, N. T., Heldebrant, M. P., Vroman, B. T., Smith, B. D., Karp, J. E., Eyck, C. J., Erlichman, C., Kaufmann, S. H., and Karnitz, L. M. (2005) Heat shock protein 90 inhibition sensitizes acute myelogenous leukemia cells to cytarabine. *Blood* **106,** 318–327
70. Pang, Y. P., Dai, H., Smith, A., Meng, X. W., Schneider, P. A., and Kaufmann, S. H. (2012) Bak conformational changes induced by ligand binding. Insight into BH3 domain binding and Bak homo-oligomerization. *Sci. Rep.* **2,** 257
71. Hornak, V., Abel, R., Okur, A., Strockbine, B., Roitberg, A., and Simmerling, C. (2006) Comparison of multiple Amber force fields and development of improved protein backbone parameters. *Proteins* **65,** 712–725
72. Wickstrom, L., Okur, A., and Simmerling, C. (2009) Evaluating the performance of the ff99SB force field based on NMR scalar coupling data. *Biophys. J.* **97,** 853–856
73. Berendsen, H. J. C., Postma, J. P. M., van Gunsteren, W. F., Di Nola, A., and Haak, J. R. (1984) Molecular dynamics with coupling to an external bath. *J. Chem. Phys.* **81,** 3684–3690
74. Darden, T. A., York, D. M., and Pedersen, L. G. (1993) Particle Mesh Ewald. An N log(N) method for Ewald sums in large systems. *J. Chem. Phys.* **98,** 10089–10092
75. Gavathiotis, E., Suzuki, M., Davis, M. L., Pitter, K., Bird, G. H., Katz, S. G., Tu, H. C., Kim, H., Cheng, E. H., Tjandra, N., and Walensky, L. D. (2008) BAX activation is initiated at a novel interaction site. *Nature* **455,** 1076–1081
76. Dewson, G., Kratina, T., Sim, H. W., Puthalakath, H., Adams, J. M., Colman, P. M., and Kluck, R. M. (2008) To trigger apoptosis, Bak exposes its BH3 domain and homodimerizes via BH3. Groove interactions. *Mol. Cell* **30,** 369–380
77. Killian, B. J., Kravitz, J. Y., Somani, S., Dasgupta, P., Pang, Y. P., and Gilson, M. K. (2009) Configurational entropy in protein-peptide binding. Computational study of Tsg101 ubiquitin E2 variant domain with an HIV-derived PTAP nonapeptide. *J. Mol. Biol.* **389,** 315–335
78. Dai, H., Meng, X. W., Lee, S.-H., Schneider, P. A., and Kaufmann, S. H. (2009) Context-dependent Bcl-2/Bak interactions regulate lymphoid cell apoptosis. *J. Biol. Chem.* **284,** 18311–18322
79. Ding, H., Hackbarth, J., Schneider, P. A., Peterson, K. L., Meng, X. W., Dai, H., Witzig, T. E., and Kaufmann, S. H. (2011) Cytotoxicity of farnesyltransferase inhibitors in lymphoid cells mediated by MAPK pathway inhibition and Bim upregulation. *Blood* **118,** 4872–4881

Cell Biology:

Evaluation of the BH3-only Protein Puma as a Direct Bak Activator

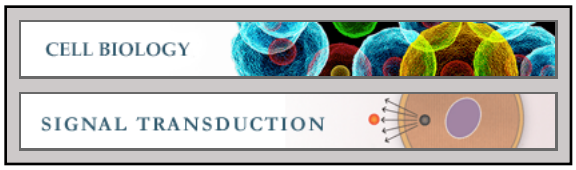

Haiming Dai, Yuan-Ping Pang, Marina Ramirez-Alvarado and Scott H. Kaufmann

J. Biol. Chem. 2014, 289:89-99.
doi: 10.1074/jbc.M113.505701 originally published online November 21, 2013